EuroSun2026

IMPACT OF METEOROLOGICAL DATASET SELECTION ON PHOTOVOLTAIC PERFORMANCE MODELLING: A CANADIAN CASE STUDY

Erin M. Tonita[1, *], D. A. Bardy[1,2], Galen Richardson[1,3], Lucio Mesquita[1]

[1] CanmetENERGY – Ottawa, Natural Resources Canada, Ottawa, Ontario, Canada
[2] Department of Mechanical and Aerospace Engineering, Carleton University, Ottawa, Ontario, Canada
[3] Department of Geography, Environment, and Geomatics, University of Ottawa, Ottawa, Ontario, Canada

Corresponding author email: erin.tonita@nrcan-rncan.gc.ca

Summary

Selection of meteorological input data can materially affect photovoltaic (PV) performance modelling and, consequently, system design, project feasibility, and bankability. In this study, we validated three satellite-derived irradiance datasets, the Canadian Weather Energy and Engineering Datasets (CWEEDS), NASA POWER, and the National Solar Radiation Database Physical Solar Model (NSRDB PSM4), at four research-grade Canadian ground stations spanning 45.6°N to 82.5°N. Global horizontal irradiance (GHI), direct normal irradiance (DNI), and diffuse horizontal irradiance (DHI) were evaluated using root mean square error (RMSE) and mean bias error (MBE). The resulting irradiance-component biases were then propagated through identical PV models for 45°-tilt fixed arrays and single-axis tracking (SAT) arrays. Across the evaluated model-station pairs, hourly GHI RMSE ranged from 60-111 W/m^2, while DNI RMSE ranged from 132-235 W/m^2. GHI was underestimated in all cases except for NASA POWER at Alert (82.5°N), with MBE ranging from -24 W/m^2 to +12 W/m^2. DNI MBE was more variable, ranging from -51 W/m^2 to +58 W/m^2. The combined irradiance-component biases produced hourly energy yield biases ranging from -4.7 to +3.8 Wh per 100 Wp for fixed-tilt PV and from -3.2 to +7.0 Wh per 100 Wp for SAT PV. No single dataset performed best at every location or for both PV configurations. The results demonstrate that dataset suitability depends on location and array geometry, and that component-level biases can combine or offset during transposition and electrical conversion.

Keywords: Solar resource, irradiance validation, photovoltaic modelling, satellite data, uncertainty propagation, Canada

Field of application for the findings: Solar Resources and Energy Meteorology

Addressed audience: solar resource researchers; PV modellers (industry and academic)

1. Introduction

Reliable irradiance data is essential for photovoltaic (PV) resource assessment, system design, and performance prediction. However, research-grade ground measurements remain spatially sparse, particularly in northern and remote regions. Gridded satellite products provide broader geographical and temporal coverage, but their accuracy varies with geographic location, atmospheric conditions, and depends on the irradiance component being modelled. Errors can be particularly pronounced over complex terrain, under cloudy conditions, in the presence of snow, and at low solar elevation angles (Forstinger et al., 2023; Suri and Cebecauer, 2024), all of which are relevant to PV modelling in Canada and other high latitude regions.

The importance of meteorological dataset selection extends beyond solar-resource characterization as errors in irradiance inputs propagate through irradiance transposition, module-temperature calculations, electrical performance models, and inverter models. The magnitude and direction of the resulting PV energy yield error will depend on the individual biases in global horizontal irradiance (GHI), direct normal irradiance (DNI), and diffuse horizontal irradiance (DHI), and the geometry of the PV array.

Previous studies have demonstrated that the choice of solar resource dataset can affect PV energy yield predictions and system design. For example, AlFaraj *et al.* (2024) found that PV modelling conducted with satellite data showed higher mean absolute percentage error (3.4-27.2%) than modelling conducted with ground data (1.5-3.5%) in six locations in Ireland. Dekker *et al.* (2012) showed that the choice of irradiance dataset affected PV system and battery energy storage sizing for a system designed in South Africa, with satellite data resulting in the PV system being undersized by 8%. Ernst *et al.* (2016) showed that the choice of input data can be critical to the accuracy of energy yield predictions by comparing predicted PV yield using satellite and ground data in five locations in Australia.

Although the effects of meteorological dataset selection have been examined elsewhere, fewer studies have traced component-level irradiance biases through PV performance models and reported results over the wide range of latitudes and climatic conditions in Canada. This limitation is especially pronounced in the Canadian Arctic, where ground observations are scarce and irradiance retrieval is complicated by low solar elevation angles, seasonal snow cover, high surface albedo, persistent cloud, and extended periods of polar night and midnight sun.

In this study, we evaluate three meteorological datasets against quality-controlled measurements from four research-grade Canadian stations spanning 45.6°N to 82.5°N: Varennes, Quebec; Regina, Saskatchewan; Eureka, Nunavut; and Alert, Nunavut. The four stations provide a geographically and climatically diverse test set, including humid continental climates and high Arctic polar climates. We evaluated the Canadian Weather Energy and Engineering Datasets (CWEEDS), NASA Prediction of Worldwide Energy Resources (NASA POWER), and the National Solar Radiation Database Physical Solar Model version 4 (NSRDB PSM4). Hourly GHI, DNI, and DHI from each dataset were evaluated against coincident ground measurements using root mean square error (RMSE) and mean bias error (MBE). Finally, the observed irradiance-component biases are propagated through identical PV modelling workflows for a south-facing, 45°-tilt fixed array and a horizontal single-axis tracking (SAT) array.

2. Methodology

2.1. Irradiance Model Validation

CWEEDS, NASA POWER, and PSM4 satellite-derived irradiance datasets were evaluated by comparing their hourly irradiance estimates with quality-controlled measurements from four research-grade Canadian ground stations. The stations span approximately 37° of latitude and include two southern Canadian sites, Varennes and Regina, and two high Arctic sites, Eureka and Alert. Their locations are shown in Figure 1, and the station coordinates, elevations, measurement networks, and analysis periods are summarized in Table 1. Three of the four stations collected data as a part of the Baseline Surface Radiation Network (BSRN) (Driemel et al., 2018). The station in Varennes is operated by Natural Resources Canada.

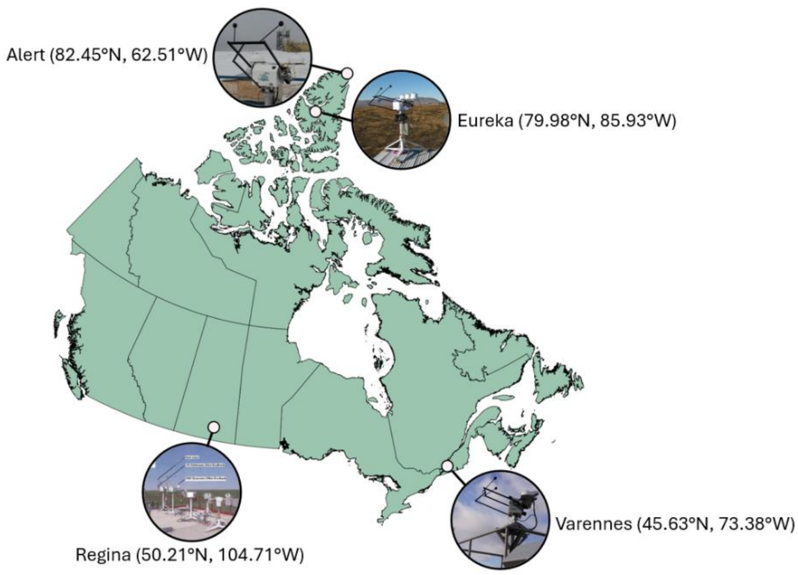

Figure 1: High-quality ground stations in Canada used in this study.

Ground measurements were quality controlled using procedures outlined in Forstinger *et al.* (2021). Only records that passed quality control were retained for analysis. Comparisons were conducted over the available multi-year period at each station, as listed in Table 1. All statistics were calculated from temporally aligned hourly averaged values.

Table 1. High-quality Canadian ground station data.

Station Name	Network	Latitude, Longitude	Elevation (m)	Data Period Analyzed
Varennes, QC	NRCan	45.63°N, 73.38°W	24	2017-2023
Regina, SK	BSRN	50.21°N, 104.71°W	587	2001-2011
Eureka, NU	BSRN	79.98°N, 85.93°W	85	2007-2011
Alert, NU	BSRN	82.45°N, 62.51°W	127	2005-2013

The geographic coverage and spatial resolution of CWEEDS, NASA POWER, and PSM4 datasets are summarized in Table 2. PSM4 was evaluated only at Varennes and Regina due to Arctic data availability limitations, whereas CWEEDS and NASA POWER were evaluated at all four stations.

Table 2. Summary of meteorological datasets.

Model Name	Model Abbrev.	Organization	Coverage	Spatial Resolution	Years Covered
Canadian Weather Energy and Engineering Datasets	CWEEDS	NRCan	Canada	649 sites	1998-2023
Prediction of Worldwide Energy Resources	NASA POWER	NASA	Global	Solar variables: 1° x 1° Other: 0.625° x 0.5°	2001-present
Physical Solar Model v4	PSM4	NLR NSRDB	USA & Americas, <60°N	4 km	1998-2023
			Polar region ≥60°N	4 km	2013-2023

For each available dataset-station pair, modelled GHI, DNI, and DHI were compared with the corresponding ground measurements. Hourly validation metrics were calculated for RMSE and MBE following Equations 1 and 2:

$$RMSE = \sqrt{\frac{1}{N}\sum_{i=1}^{N}\left(x_{D,i} - x_{G,i}\right)^2} \qquad \text{(Eq. 1)}$$

$$MBE = \frac{1}{N}\sum_{i=1}^{N}\left(x_{D,i} - x_{G,i}\right) \qquad \text{(Eq. 2)}$$

where N is the number of timestamps, x_D is the meteorological dataset irradiance, and x_G is the measured ground irradiance. x = GHI, DNI, or DNI.

RMSE characterizes the overall magnitude of hourly irradiance differences and gives greater weight to large errors. MBE characterizes systematic overestimation or underestimation, where a positive MBE indicates that the meteorological dataset overestimated ground irradiance and a negative MBE indicates an underestimation of ground irradiance.

2.2. PV Modelling

Following the irradiance dataset validation, we evaluated how component-level biases propagated through the PV modelling chain at each station. We simulated the performance of two PV configurations: a fixed-tilt array and a horizontal single-axis tracker (SAT). The same system specifications were applied to the simulations driven by ground measurements and those driven by meteorological datasets. The fixed-tilt array was oriented due south with a tilt of 45° at all four stations to avoid over-emphasizing ground irradiance in simulation output at high Arctic locations. The SAT system was oriented to track from the east to the west.

To account for sky anisotropy, plane-of-array (POA) irradiance was calculated using the Perez sky diffuse model (Perez *et al*., 1990). The array geometry and associated irradiance transposition were calculated with pvfactors within a pvlib modelling workflow (Jensen et al., 2023). The simulated module was a monofacial 715 Wp Canadian Solar module selected from the System Advisor Model California Energy Commission module database. Module electrical performance was calculated using the California Energy Commission 6-parameter single-diode model (Dobos, 2012). Cell temperature was estimated using the Ross temperature model, which relates module or cell temperature to ambient temperature and incident irradiance.

Hourly DC power was calculated for each quality-controlled timestep over the complete multi-year analysis period available at each station. DC power was converted to AC power using the PVWatts inverter model. A fixed DC-to-AC ratio of 1.2 and a nominal inverter efficiency of 96% were applied to both PV configurations. Hourly AC energy yield was obtained by integrating the simulated AC power over each hourly interval.

The MBE between the meteorological dataset simulation and the corresponding ground-reference simulation was calculated for hourly POA and AC energy yield. Energy yield results were normalized by module rated power and expressed per 100 Wp of installed capacity: $(MBE_{EY}/P_{rated}) \times 100$ Wp.

3. Results

3.1. Irradiance Model Validation

The results of the hourly meteorological dataset validation work are shown in Table 3 for GHI, DNI, and DHI. MBE for GHI, DNI, and DHI table cells are coloured by their sign. Across all evaluated model-station combinations, GHI RMSE ranged from 60 to 111 W/m², DHI RMSE from 51 to 86 W/m², and DNI RMSE from 132 to 235 W/m². DNI exhibited the largest absolute hourly errors at every station.

Systematic GHI biases were predominantly negative. CWEEDS underestimated GHI at all four stations, with MBE ranging from −12 W/m² at Varennes to −20 W/m² at Eureka. NASA POWER also underestimated GHI at Varennes, Regina, and Eureka, but overestimated it by 12 W/m² at Alert. PSM4 had the smallest GHI bias at Varennes, −2 W/m², but the largest negative GHI bias among the evaluated southern-site cases at Regina, −24 W/m². Thus, the dataset with the smallest GHI bias depended on location: PSM4 at Varennes, and NASA POWER at Regina, Eureka, and Alert.

Table 3. Summary of validation statistics.

Model	Station	GHI RMSE (W/m^2)	DNI RMSE (W/m^2)	DHI RMSE (W/m^2)	GHI MBE (W/m^2)	DNI MBE (W/m^2)	DHI MBE (W/m^2)
CWEEDS	Varennes (45.6°N)	78	132	65	-12	4	-5
	Regina (50.2°N)	97	202	67	-17	6	-15
	Eureka (80.0°N)	73	214	51	-20	-14	-8
	Alert (82.5°N)	79	235	68	-18	42	-31
PSM4	Varennes (45.6°N)	82	159	63	-2	30	-8
	Regina (50.2°N)	111	196	86	-24	-12	-16
	Varennes (45.6°N)	83	165	63	-16	2	-6

NASA POWER	Regina (50.2°N)	83	187	67	-8	-4	7
	Eureka (80.0°N)	66	210	54	-18	-51	15
	Alert (82.5°N)	60	207	53	12	58	4

DNI bias varied more strongly in both magnitude and sign. At Varennes, DNI MBE was positive for all three datasets, ranging from +2 W/m² for NASA POWER to +30 W/m² for PSM4. At Regina, biases were relatively small, ranging from −12 to +6 W/m². At the Arctic stations, the differences were larger. NASA POWER underestimated DNI at Eureka by 51 W/m² but overestimated it at Alert by 58 W/m². CWEEDS performed marginally better, and underestimated DNI by 14 W/m² at Eureka and overestimated it by 42 W/m² at Alert. These bias reversals between the two northern stations indicate that model performance cannot be inferred from latitude alone and may also depend on local cloud, atmospheric, surface-albedo, and terrain conditions.

DHI biases were smaller than GHI and DNI biases, but remain important because diffuse irradiance contributes to tilted-plane irradiance, particularly under cloudy conditions and at high solar zenith angles. The largest negative DHI bias was observed for CWEEDS at Alert, −31 W/m². In several cases, biases in the three irradiance components had opposing signs, creating the potential for partial cancellation when irradiance was transposed to the plane of the array.

3.2. PV Modelling

To determine how biases in individual irradiance components propagate into PV model outcomes, PV modelling was undertaken using pvlib for a fixed-tilt system and a SAT system. Figures 2 to 5 and Table 4 show how the irradiance-component biases propagated through the PV modelling chain. The response was neither uniform across sites nor directly proportional to GHI bias. Instead, the resulting POA irradiance and energy yield biases reflected the combined effects of GHI, DNI, and DHI errors, array geometry, solar position, irradiance transposition, and the nonlinear electrical response of the PV model.

At Varennes, all three datasets produced relatively small energy yield biases (< 2 Wh per 100 Wp) despite differences in their component-level irradiance errors. CWEEDS and PSM4 fixed-tilt energy yield biases were +0.35 and +0.83 Wh per 100 Wp, respectively, and their SAT biases were +0.53 and +0.33 Wh per 100 Wp. NASA POWER had an almost unbiased GHI estimate, −2 W/m², but overestimated DNI by 30 W/m². This produced the largest positive energy yield biases at the site: +1.27 Wh per 100 Wp for the fixed-tilt system and +1.47 Wh per 100 Wp for the SAT system. The Varennes results demonstrate that a small GHI bias does not guarantee a correspondingly small PV-model bias due to the importance with other irradiance components on a tilted plane.

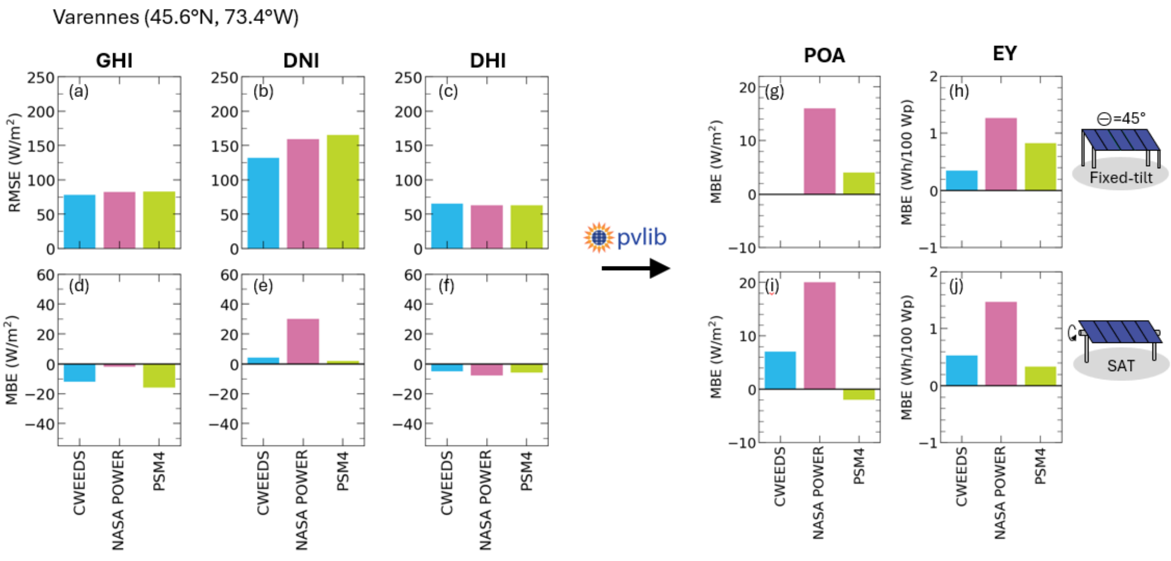

Figure 2: RMSE (a-c) and MBE (d-f) for GHI, DNI, and DHI irradiance components in Varennes, and the resulting fixed-tilt PV MBE for (g) POA and (h) energy yield and SAT PV MBE for (i) POA and (j) energy yield.

In Regina, dataset selection had a larger effect on modelled energy yield. PSM4 had the smallest absolute fixed-tilt and SAT energy yield biases, +1.31 and +0.91 Wh per 100 Wp, respectively. CWEEDS produced negative biases of −0.66 Wh per 100 Wp for the fixed-tilt system and −1.65 Wh per 100 Wp for the SAT system. NASA POWER produced the largest underestimation, with −4.74 Wh per 100 Wp for fixed-tilt and −3.22 Wh per 100 Wp for SAT, due to all three component biases having the same sign.

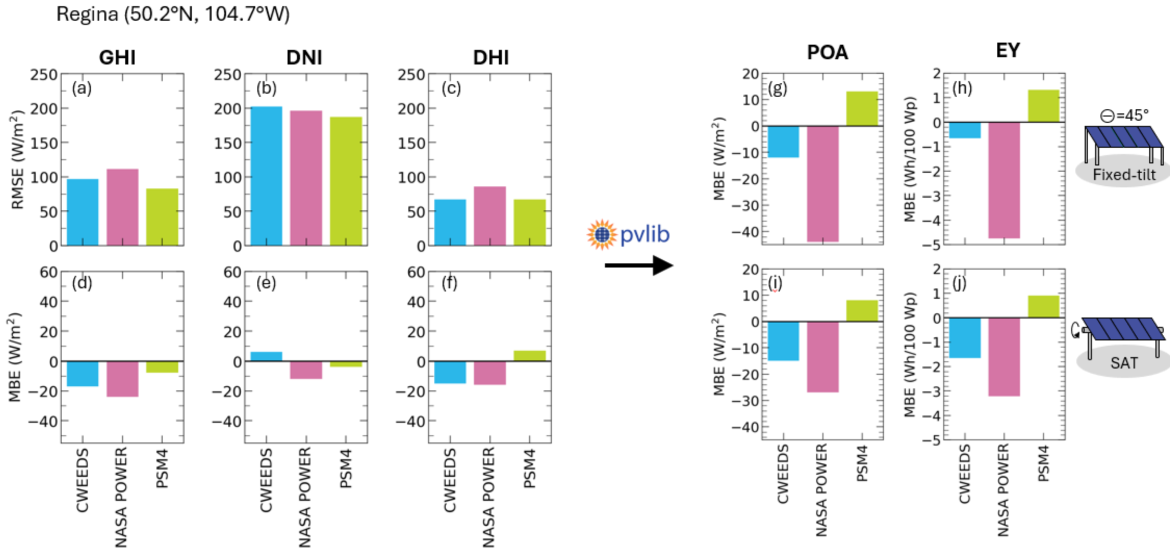

Figure 3: RMSE (a-c) and MBE (d-f) for GHI, DNI, and DHI irradiance components in Regina, and the resulting fixed-tilt PV MBE for (g) POA and (h) energy yield and SAT PV MBE for (i) POA and (j) energy yield.

At Eureka, both evaluated datasets underestimated GHI and DNI. CWEEDS underestimated all three irradiance components and consequently produced energy yield biases of −1.11 Wh per 100 Wp for fixed-tilt and −1.43 Wh per 100 Wp for SAT. NASA POWER underestimated GHI and DNI and overestimated DHI, with opposing component biases resulting in a small positive fixed-tilt bias of +0.37 Wh per 100 Wp and a negative SAT bias of −0.63 Wh per 100 Wp. This contrast illustrates that the diffuse component can partially compensate for direct-beam underestimation in a fixed array, whereas the tracking configuration remains more sensitive to DNI.

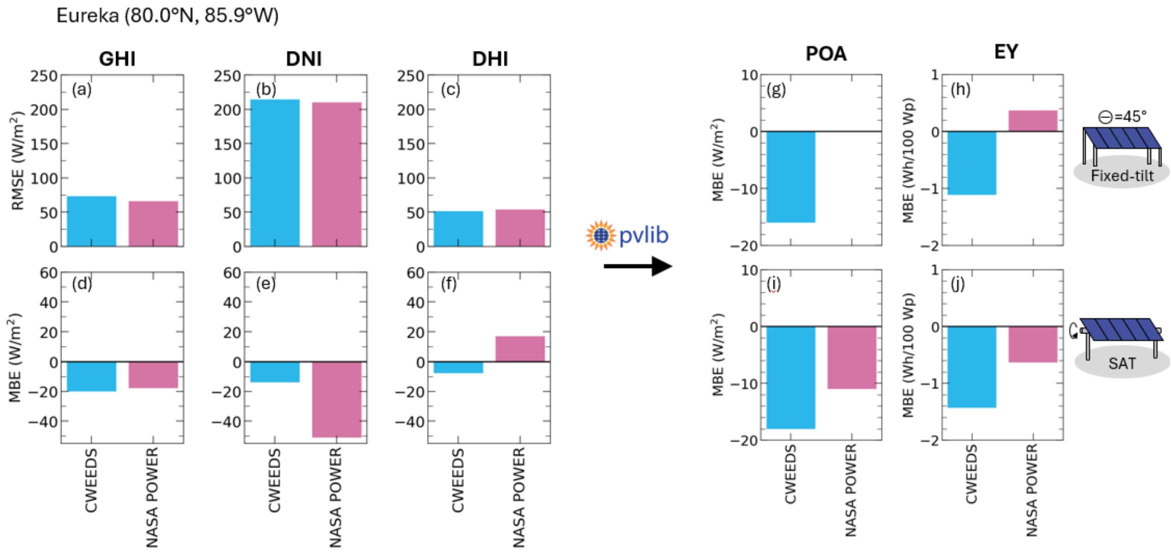

Figure 4: RMSE (a-c) and MBE (d-f) for GHI, DNI, and DHI irradiance components in Eureka, and the resulting fixed-tilt PV MBE for (g) POA and (h) energy yield and SAT PV MBE for (i) POA and (j) energy yield.

The largest positive energy yield bias occurred for NASA POWER at Alert, with energy yield biases of +3.75 Wh per 100 Wp for fixed-tilt and +7.01 Wh per 100 Wp for SAT. As a contrast, component bias compensation in CWEEDS led to energy yield biases of −1.36 Wh per 100 Wp for fixed-tilt and +0.10 Wh per 100 Wp for

SAT. For the tracker, the positive DNI contribution almost completely offset the negative global and diffuse biases for CWEEDS.

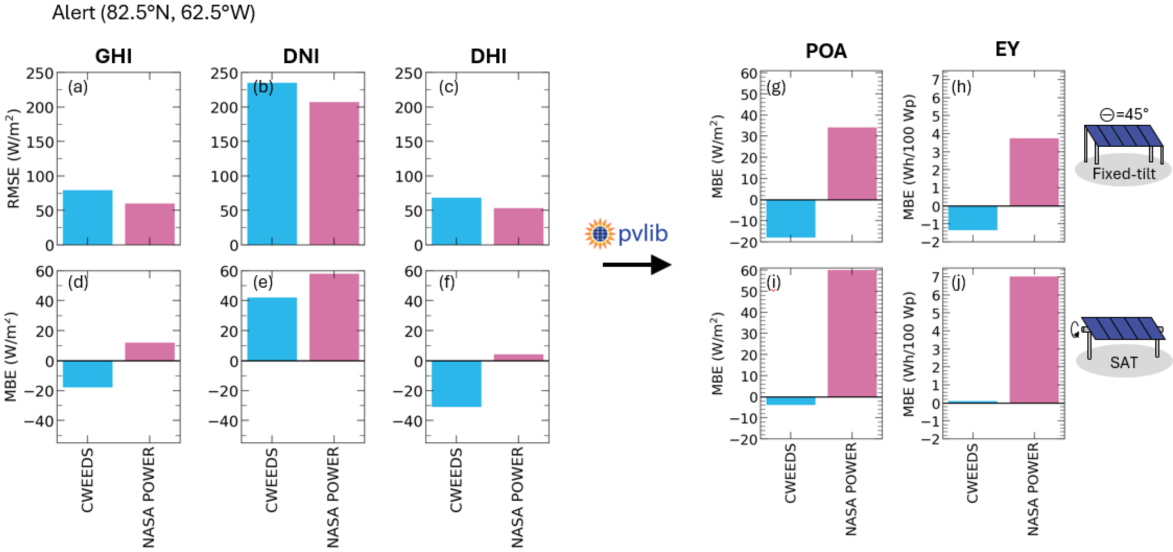

Figure 5: RMSE (a-c) and MBE (d-f) for GHI, DNI, and DHI irradiance components in Alert, and the resulting fixed-tilt PV MBE for (g) POA and (h) energy yield and SAT PV MBE for (i) POA and (j) energy yield.

Across all cases, fixed-tilt hourly energy yield MBE ranged from −4.74 to +3.75 Wh per 100 Wp, while SAT energy yield MBE ranged from −3.22 to +7.01 Wh per 100 Wp. The largest absolute fixed-tilt bias occurred for PSM4 at Regina, whereas the largest absolute SAT bias occurred for NASA POWER at Alert. No dataset consistently minimized energy yield bias across all locations and both system configurations. Biases with the same sign across GHI, DNI, and DHI reinforced one another, while biases with opposing signs could partially cancel during POA transposition. SAT results were generally more sensitive to large DNI biases, although the magnitude of that response also depended on accompanying GHI and DHI errors. Consequently, validation based only on GHI may not adequately characterize the uncertainty introduced into PV simulations, particularly for tracking systems.

Table 4. Summary of irradiance component bias propagation into hourly POA and energy yield bias.

Model	Station	GHI MBE (W/m^2)	DNI MBE (W/m^2)	DHI MBE (W/m^2)	Model energy yield bias compared to model results using ground data (Wh / 100 Wp)	
					Fixed-tilt PV	SAT PV
CWEEDS	Varennes (45.6°N)	-12	4	-5	0.35	0.53
	Regina (50.2°N)	-17	6	-15	-0.66	-1.65
	Eureka (80.0°N)	-20	-14	-8	-1.11	-1.43
	Alert (82.5°N)	-18	42	-31	-1.36	0.1
PSM4	Varennes (45.6°N)	-2	30	-8	1.27	1.47
	Regina (50.2°N)	-24	-12	-16	-4.74	-3.22
NASA POWER	Varennes (45.6°N)	-16	2	-6	0.83	0.33
	Regina (50.2°N)	-8	-4	7	1.31	0.91
	Eureka (80.0°N)	-18	-51	15	0.37	-0.63
	Alert (82.5°N)	12	58	4	3.75	7.01

4. Conclusion

This study quantified how the selection of meteorological data affects irradiance transposition and PV performance modelling accuracy by tracing irradiance component bias through simple PV models in four Canadian locations. Hourly GHI RMSE ranged from 60 to 111 W/m², while DNI RMSE ranged from 132 to 235 W/m². GHI was underestimated in nearly all cases, but DNI and DHI biases varied substantially in both magnitude and sign. These component-level differences propagated through POA transposition and electrical conversion, producing fixed-tilt energy yield biases from −4.74 to +3.75 Wh per 100 Wp and SAT biases from −3.22 to +7.01 Wh per 100 Wp. No single dataset provided the lowest irradiance or energy yield error at every site; CWEEDS tended to have the lowest resulting energy yield bias for fixed-tilt PV, while NASA POWER tended to have the lowest bias for SAT PV.

These findings show that GHI validation alone is insufficient for selecting meteorological data for PV performance studies. DNI and DHI must also be evaluated because component errors can reinforce or compensate for one another after transposition. This is particularly important for tracking systems, whose performance is more sensitive to direct-beam irradiance. A small final energy yield bias should also not be interpreted automatically as a result of high dataset accuracy because it may result from cancellation among larger irradiance-component biases, such as with NASA POWER in Eureka.

This work highlights the need for further comprehensive studies on meteorological dataset accuracy across a wider range of locations in Canada, to determine trends and best practices for PV applications. Where possible, candidate datasets should be validated against quality-controlled measurements using both bias and scatter metrics before being used for design or resource assessment in a region. The larger and less consistent errors observed at the Arctic stations suggests a need for further expansion and long-term maintenance of research-grade irradiance measurements in northern Canada. Such observations are needed both to characterize uncertainty in present-day PV assessments and to improve future satellite and reanalysis products for high-latitude environments.

5. References

AlFaraj, J., Popovici, E., and Leahy, P., "Solar irradiance database comparison for PV system design: A case study," *Sustainability*, 16, 6436 (2024). https://doi.org/10.3390/su16156436

Dekker, J., Nthontho, M., Chowdhury, S., and Chowdhury, S. P., "Investigating the effects of solar modelling using different solar irradiation data sets and sources within South Africa," *Solar Energy*, 86(9), pp. 2354-2365 (2012). https://doi.org/10.1016/j.solener.2012.05.007

Dobos, A. P., "An Improved Coefficient Calculator for the California Energy Commission 6 Parameter Photovoltaic Module Model", *Journal of Solar Energy Engineering*, 134(2) (2012). https://doi.org/10.1115/1.4005759

Driemel, A., Augustine, J., Behrens, K., *et. al.*, "Baseline surface radiation network (BSRN): structure and data description (1992–2017)", *Earth System Science Data*, 10(3):1491–1501 (2018). https://doi.org/10.5194/essd-10-1491-2018

Ernst, M., Thomson, A., Haedrich, I., and Blakers, A., "Comparison of ground-based and satellite-based irradiance data for photovoltaic yield estimation," *Energy Procedia*, 92, pp. 546-553 (2016). https://doi.org/10.1016/j.egypro.2016.07.139

Forstinger, A., Wilbert, S., Jensen, A. R., *et al.*, "Worldwide benchmark of modelled solar irradiance data," Report IEA-PVPS T16-05:2023, pp. 1-40 (2023).

Forstinger, A. *et al.*, "Expert quality control of solar radiation ground data sets," *Proceedings of SWC 2021: ISES Solar World Congress*, 1037-1048 (2021). https://doi.org/10.18086/swc.2021.38.02

Jensen, A. R., Anderson, K. S., Holmgren, W. F., Mikofski, M. A., Hansen, C. W., Boeman, L. J., and Loonen, R., "pvlib iotools – Open-source Python functions for seamless access to solar irradiance data," *Solar Energy*, 266, 112092 (2023). https://doi.org/10.1016/j.solener.2023.112092

Natural Resources Canada, "Meteorological station at CanmetENERGY-Varennes," Program of Energy

Research and Development. https://natural-resources.canada.ca/energy-efficiency/building-energy-efficiency/testing-facilities

Perez, R., Ineichen, P., Seals, R., Michalsky, J., and Stewart, R., "Modeling daylight availability and irradiance components from direct and global irradiance," *Solar Energy*, 44 (5), 271-289 (1990). https://doi.org/10.1016/0038-092X(90)90055-H

Suri, M., and Cebecauer, T., "Solargis solar resource database: validation of satellite-based solar radiation model," Solargis Reference No. 170-18/2024, pp.1-63 (2024).